Available online at www.sciencedirect.com
ScienceDirect
Earth and Planetary Science Letters 261 (2007) 500–516
EPSL
www.elsevier.com/locate/epsl

Brief thermal pulses during mountain building recorded by Sr diffusion in apatite and multicomponent diffusion in garnet

Jay J. Ague [a,*], Ethan F. Baxter [b]

[a] Department of Geology and Geophysics, Yale University, P.O. Box 208109, New Haven, CT 06520-8109, USA
[b] Department of Earth Sciences, Boston University, 685 Commonwealth Ave., Boston, MA 02215, USA

Received 15 March 2007; received in revised form 5 June 2007; accepted 10 July 2007
Available online 19 July 2007
Editor: C.P. Jaupart

Abstract

We use the records of Sr diffusion preserved in apatite and corroborating multicomponent Fe-Mg–Ca–Mn diffusion preserved in garnet from the classic Barrovian metamorphic zones (Scotland) to quantify the timescale for the thermal peak of crustal heating c. 465 Ma. We show that Sr diffusion in apatite is a powerful means to determine thermal timescales, and provide the first set of diffusion-based timescale estimates across a wide range of metamorphic grades for Barrovian metamorphism. The results demonstrate that the thermal peak was extremely brief and lasted a few hundred thousand years. This timescale is one to two orders of magnitude shorter than peak timescales predicted by conventional models based on conductive relaxation of overthickened crust. The short peak thermal pulse or pulses probably involved advective heat transfer driven by magmas and associated fluid flow, followed by rapid exhumation. Peak thermal pulses may represent a very short part (<1 Ma) of overall mountain building cycles lasting ~10^7 yr or more, but play a dominant role in determining mineralogy, geochemical fluxes, and fluid production in mountain belts.

Keywords: diffusion; Barrovian; Scotland; apatite; garnet; thermal history

1. Introduction

Profound questions surround the timescales, rates, and mechanisms of heat transfer through Earth's crust required to drive chemical reactions that produce metamorphic rocks and liberate fluids during plate convergence and mountain building (Chamberlain and Rumble, 1988; Baxter and DePaolo, 2000; Camacho et al., 2005; Kelly, 2005; Wilbur and Ague, 2006; Bjornerud and Austrheim, 2006). Frequently cited models of conductive thermal relaxation in tectonically overthickened crust predict that attainment of peak (maximum temperature) conditions should span ~10 million years or more across collisional orogenic belts (Thompson and England, 1984). However, recent work in the Barrovian type locality (Scotland) and in related rocks in Ireland suggests much shorter timescales (Friedrch et al., 1999; Oliver et al., 2000; Baxter et al., 2002) which may have resulted from advective magmatic heating and associated fluid flow ~465 million years ago (Baxter et al., 2002). This result has broad implications because Barrovian metamorphic sequences are the most commonly recognized type in mountain belts worldwide.

Very precise estimates of the duration of heating are required to determine mechanisms of heat transfer and tectonism, but conventional radiometric dating methods

* Corresponding author.
E-mail address: jay.ague@yale.edu (J.J. Ague).

0012-821X/$ - see front matter © 2007 Elsevier B.V. All rights reserved.
doi:10.1016/j.epsl.2007.07.017

have typical uncertainties of several million years or more for rocks of this age. However, the record of diffusion preserved within minerals has the potential to resolve extremely short-lived events. Diffusion is a thermally-activated process that operates to smooth compositional heterogeneities within crystals. Thus, preservation of pre-existing heterogeneities constrains the timescales of thermal events, if diffusion rates, temperature, and initial concentration profiles are well constrained (Watson et al., 1985; Cherniak and Ryerson, 1993; Lasaga and Jiang, 1995; Ganguly et al., 1996; van Haren et al., 1996; Carlson and Schwarze, 1997; Graham et al., 1998; Dachs and Proyer, 2002; Faryad and Chakraborty, 2005). For example, diffusive profiles in garnet have been used to estimate retrograde cooling and exhumation rates (Lasaga and Jiang, 1995).

Recent diffusion-based results suggest that some metamorphic processes may operate over much shorter timescales than previously thought. Examples include fluid infiltration and vein formation during Barrovian metamorphism in New England (van Haren et al., 1996), fluid-triggered granulite to eclogite reaction, Holsnøy, Norway (Camacho et al., 2005), thermal pulses on Naxos, Greece (Wijbrans and McDougall, 1986), and rapid burial and/or exhumation of eclogite and associated conduction-dominated heat transfer during alpine orogenesis (Dachs and Proyer, 2002; Faryad and Chakraborty, 2005). Nonetheless, hypotheses of short-lived metamorphism have been controversial (Bjornerud and Austrheim, 2006), largely because quantitative interpretation of intracrystalline diffusion may depend on a variety of factors including: (1) compositional variations within mineral solid solutions, (2) initial and boundary conditions, (3) uncertainties in placing the observed diffusion profiles into the context of prograde, peak, and/or retrograde stages of the orogenic cycle, and (4) in some cases, the presence or absence of water. Furthermore, experimental calibrations of diffusion rates can have significant uncertainties which are often not propagated when field-based estimates of timescales are made. It begs the question whether these inferences of short-lived metamorphic processes are rare, isolated exceptions or whether they may characterize continental metamorphism in general.

We test the hypothesis of short-lived thermal pulses during typical regional metamorphism by focusing on a widespread mineral not previously considered in this regard: fluor–apatite (apatite). Sr diffusion in apatite is a very promising means to quantify timescales of thermal events, as discussed here. (1) The Sr diffusion is described by a tightly-constrained, linear Arrehnius relationship calibrated over a large T range of 550 °C (Watson et al., 1985; Cherniak and Ryerson, 1993). (2) Three different experimental techniques all produce a single, internally-consistent diffusion calibration (Watson et al., 1985; Cherniak and Ryerson, 1993). The diffusion exchange vector appears to be very predictable and may simply be: $Sr^{2+} \leftrightarrow Ca^{2+}$. (3) The diffusion coefficient (D) is calibrated down to a relatively low experimental T of 700 °C (Cherniak and Ryerson, 1993). Diffusion modeling for our samples involves only a small projection (100 to 200 °C) to lower T. It is extremely unlikely that the diffusion mechanism would change significantly over this relatively small projection range. (4) The effects of radiation damage on diffusivity are negligible at high temperatures where such damage is quickly annealed (Weber et al., 1997). (5) Natural fluor-apatites have compositions that closely approach the pure end-member (see below), so complications due to extensive solid solution are not an issue. (6) Diffusion of Sr may be weakly anisotropic (faster perpendicular to c-axis), but anisotropic effects are within experimental error (Watson et al., 1985; Farver and Giletti, 1989; Cherniak and Ryerson, 1993) and are accounted for in our data reduction. (7) Elemental (not isotopic tracer) Sr diffusion was measured experimentally (Watson et al., 1985; Cherniak and Ryerson, 1993), directly analogous to the natural Sr diffusion that we study. (8) Sr diffusion slows sufficiently below about 500 °C, so the system is effectively non-responsive to diffusive modification during most lower greenschist and sub-greenschist facies retrogression. (9) Sr concentrations can be easily determined using the electron microprobe. (10) Pressure effects should be negligible at the relatively low pressures of interest here (Farver and Giletti, 1989). (11) Apatite is a common phase that can grow during prograde metamorphism across a range of grades and persist through the peak metamorphic conditions we seek to constrain. Finally, it is worth emphasizing that diffusion timescales can be preserved in the compositions of many other minerals as well, thus providing the potential for multiple corroborating chronometers.

2. Geologic relations

Samples are from the Dalradian metasediments in Barrow's biotite (Bt), garnet (Grt), and staurolite (St) zones north of Stonehaven, and from the sillimanite (Sil) zone in the type locality near Glen Clova (Barrow, 1893; Atherton, 1977) (Fig. 1). Grt zone specimens JAB1 and JAB101L lie above the chloritoid isograd; 101L contains chloritoid crystals. Detailed sample locations and descriptions are published elsewhere (McLellan, 1985; Ague, 1997; Masters et al., 2000; Ague et al., 2001;

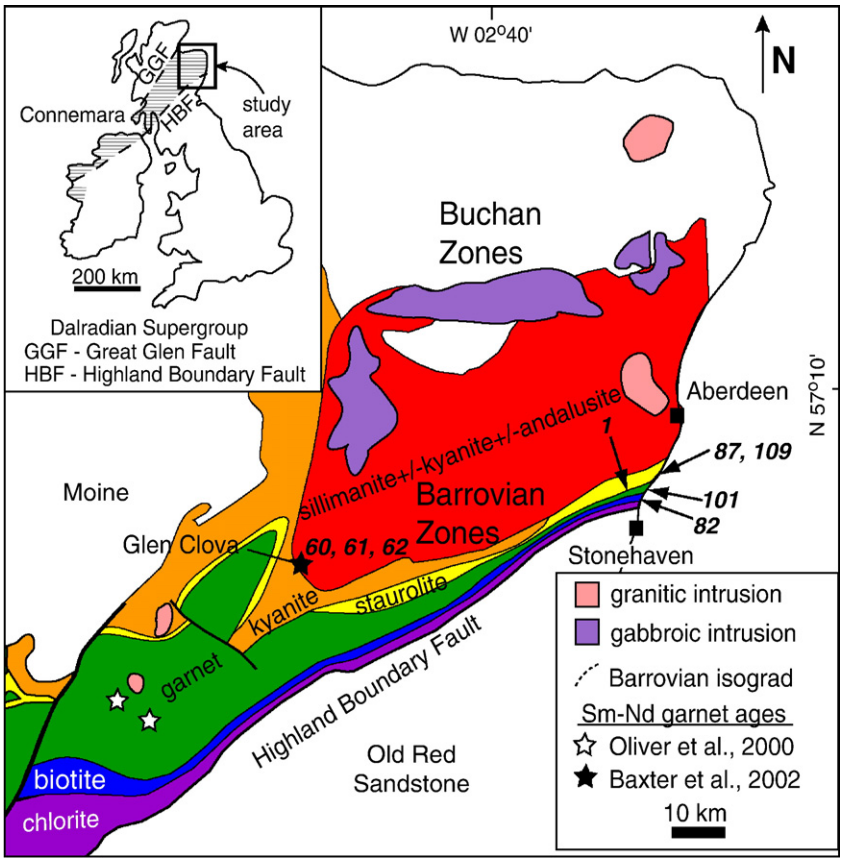

Fig. 1. Simplified map of northeast Scotland illustrating positions of the Barrovian zones and syn-metamorphic intrusions (Atherton, 1977; Ague, 1997; Masters et al., 2000; Ague et al., 2001; Baxter et al., 2002; Masters and Ague, 2005). Sample locations for this study indicated with bold italic type. All locations begin with the prefix JAB, omitted here for clarity.

Baxter et al., 2002; Masters and Ague, 2005). In many rocks, particularly in the Grt and St zones, apatite crystals have distinct, irregularly-shaped cores surrounded by rims that are elongate parallel to the dominant metamorphic foliation (Fig. 2). We interpret the cores to be relict detrital grains and the rims to be metamorphic overgrowths. Peak metamorphic porphyroblasts including garnet and staurolite overgrow this foliation and include apatite grains, so the core-rim textures in apatite must pre-date peak metamorphism and are unlikely to be retrograde features developed afterwards during cooling (see Section 5.2 below). Thus some or all of the diffusive modification of apatite core-rim zoning occurred during peak metamorphism and up until the system cooled below about 500 °C.

In order to extract timescale information, it is critical to document the compositional variations across crystals (Fig. 3). In the Bt zone, zoning of Sr is irregular and grains commonly have different Sr contents around their edges. In the Grt zone, relatively sharp steps in Sr content are apparent across core-rim boundaries. In the St zone, the profiles are smoother, but contrasts in Sr content across core-rim boundaries remain. In the Sil zone, all prograde metamorphic Sr zonation has apparently been smoothed out by diffusion and Sr contents are uniform across grains. Consequently, we model multicomponent diffusion in garnet (Carlson, 2006) to estimate the peak Sil zone timescale, because compositional heterogeneities acquired during garnet growth are still clearly evident and have not been homogenized by diffusion (Fig. 3). In summary, the progressive smoothing of Sr zonation in apatite with increasing metamorphic grade is what would be expected for diffusion operating within grains over comparable timescales.

3. Analytical methods and peak metamorphic temperatures

3.1. Imaging and electron microprobe analyses

Chemical analyses and backscattered electron images of minerals were done using the JEOL JXA-8600

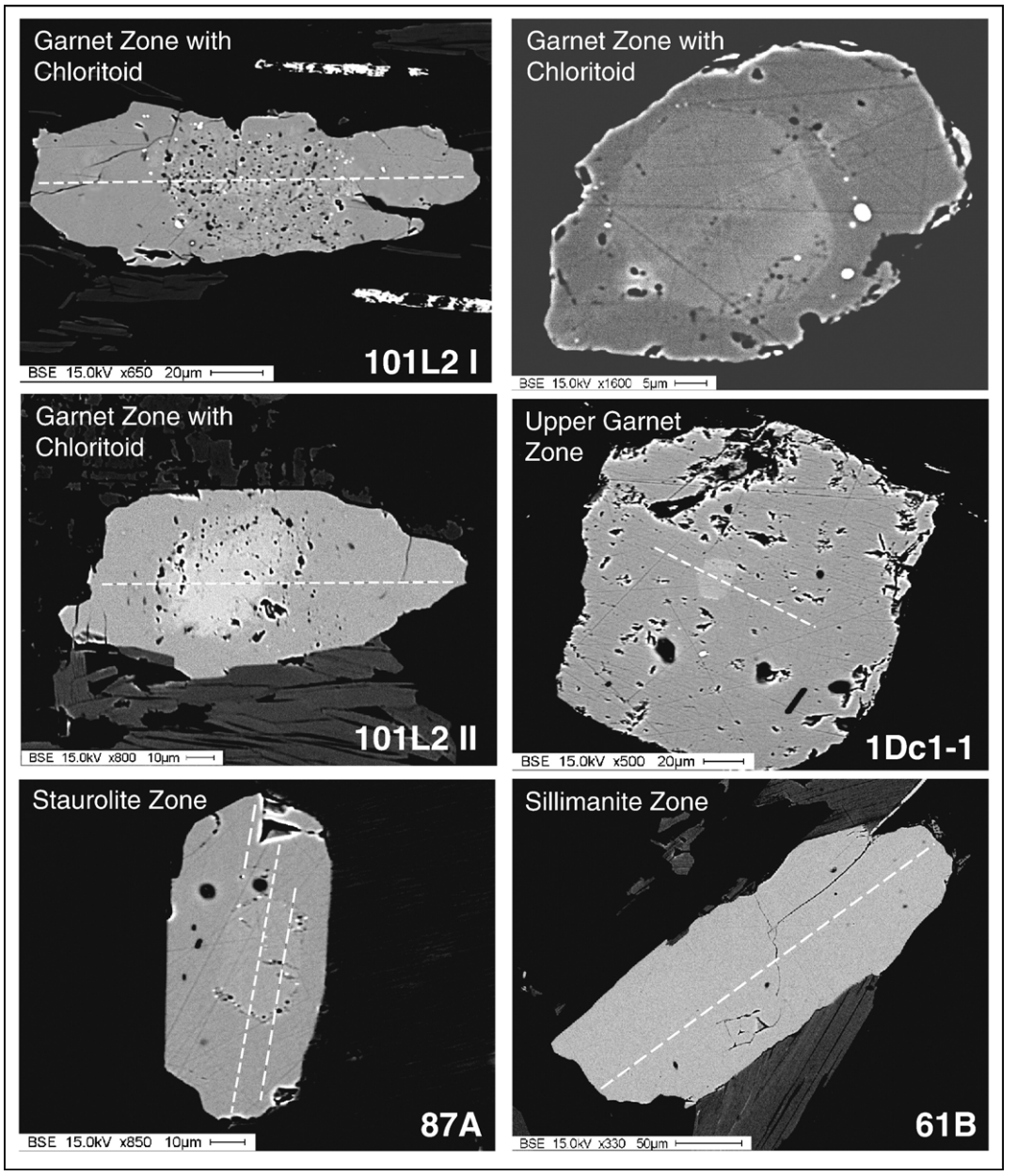

Fig. 2. Backscattered electron (BSE) images of apatite crystals. Note distinct cores and rim overgrowths for garnet and staurolite zone examples, and lack of core-rim textures in sillimanite zone example. Cores often have different backscatter contrast (gray scale) than rims; inclusions along core-rim boundaries are typically quartz (dark in images), fluid (dark), or Fe–Ti oxides (bright). Direction of grain elongation lies parallel to dominant matrix schistosity. Sample numbers for grains analyzed herein shown in lower right of images; dashed lines denote positions of Sr analysis profiles.

electron microprobe at Yale University. Analyses for Sr in apatite used 15 kV accelerating voltage, 25 nA cup beam current, wavelength-dispersive spectrometers, natural and synthetic standards, $\varphi(\rho z)$ matrix corrections, off-peak background corrections, 5 µm diameter beam spot (to minimize beam damage), 150 s on-peak counting times for Sr, and 75 s on each off-peak position. Multiple Sr determinations on unzoned Sil zone apatite crystals yield an estimated error for individual spot analyses of ±0.0087 wt.% (±2 sigma, 20 spot analyses). The calculated detection limit based on counting statistics for Sr was 0.0067 weight % (95% confidence). Trace element analyses of apatite presented in the supplemental data employed similar methods, but

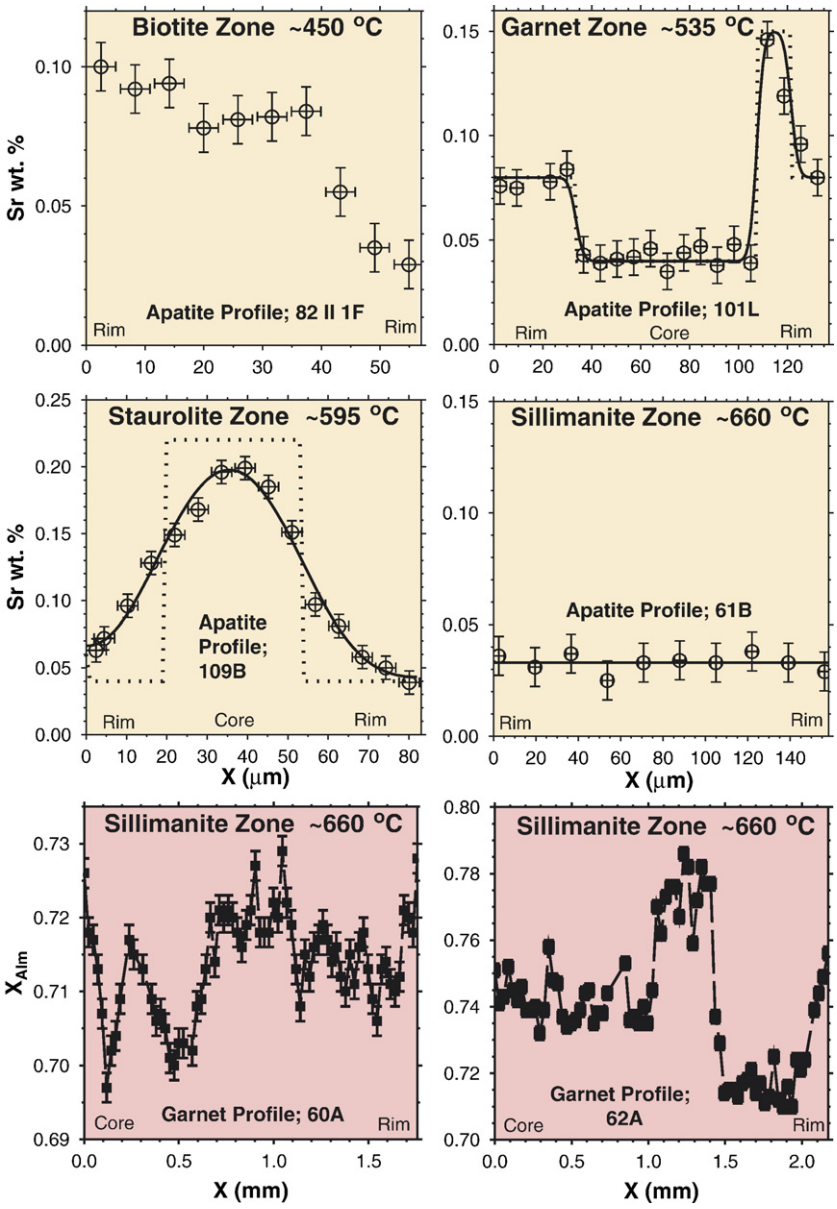

Fig. 3. Profiles of Sr across apatite crystals (four upper panels) and almandine mole fraction (X_{Alm}) across garnet (lower panels) measured using the JEOL JXA-8600 electron microprobe at Yale University. Best-fit diffusion model results for garnet and staurolite zone apatites denoted with solid lines; inferred initial step functions shown with dotted lines. Note absence of systematic zonation in biotite zone apatite, homogeneous composition of sillimanite zone apatite, and major growth zonation in both garnets. Error bars reflect 5 micrometer electron probe beam spot for apatite, and ±2 sigma analytical uncertainty for Sr and X_{Alm}.

used 20 nA beam current, and 203 second on-peak counting times. Garnet determinations used a 20 nA beam current, non-linear mean atomic number background corrections, and a focused electron beam; other parameters are described in Ague et al. (2001). As shown in the supplementary data table, analyzed cations in fluor–apatite other than Ca and P are present in minor or trace quantities.

3.2. Peak temperatures and uncertainties

For the diffusion modeling analysis we present below, rigorous evaluation of peak temperature for each sample, along with related uncertainties, is required. All temperature (T) estimates are based on garnet–biotite Fe–Mg exchange thermometry unless noted otherwise; the cited papers provide the details of the thermobarometry

calculations. The results of Ague et al. (2001) for the Glen Clova Sillimanite zone locality yield a 3 sigma uncertainty on mean peak T of ±24 °C based on ten P–T estimates. For samples collected along the northeastern coast of Scotland, we use available data for T extending north of the Highland Boundary Fault (HBF) and the town of Stonehaven (Fig. 4; see Masters and Ague, 2005 for profile location). The T estimate for the sample nearest the fault (JAB 77A) was obtained using quartz–calcite oxygen isotope thermometry (Masters et al., 2000). The increase in T northward from the fault can be described by a simple linear relationship up to the staurolite zone where no further change in peak temperature is evident (for this reason, note that for the regression analysis we combined all of the staurolite zone samples together at an x position of 1260 meters). The squared correlation coefficient for the linear fit of T versus distance from the HBF is $r^2 = 0.99$. The scatter of T data about the best-fit line can be used to estimate the T uncertainty for individual samples. The estimated 3 sigma uncertainty for the T data obtained using the normalized square root of the cumulative sum of squares is ±30 °C (Eq. 25.62 in Lawson and Hanson, 1974). Importantly, the data from Glen Clova (Ague et al., 2001) and of Fig. 4 yield similar estimates for uncertainty on peak T. To be conservative, a ±30 °C uncertainty (60 °C span) on peak T was used in all model calculations. The peak T for Grt zone sample JAB101L was 535 °C (Ague, 1997). The average St zone T of 595 °C (Masters et al., 2000) was used for samples JAB87A and JAB109B. The average T of 660 °C was used for Sil zone samples JAB60A and JAB62A (Ague et al., 2001). We used 550 °C obtained from the linear regression (Fig. 4) for sample JAB1Dc1-1 which lies in the upper greenschist facies just below the St zone (Masters and Ague, 2005). Pressure was ~0.4 GPa for the Grt and St zone examples (Ague, 1997), and 0.57 GPa for the Sil zone (Ague et al., 2001).

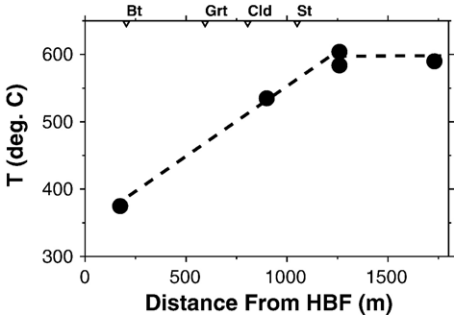

Fig. 4. Published temperature estimates for a regional profile extending north of the Highland Boundary Fault (HBF) and the town of Stonehaven. Positions of biotite (Bt), garnet (Grt), chloritoid (Cld), and staurolite (St) isograds shown with inverted triangles. See Masters and Ague (2005) for detailed profile location.

4. Diffusion modelling

4.1. General approach

Here we outline our general diffusion modelling approach for apatite and garnet. Details are then provided in the following sections. To be conservative, our calculations assume initial step functions in composition across core-rim boundaries. Taking initially smoothed profiles would result in shorter timescales. Forward modelling was used to compute the time required to relax the initial step functions to match the measured chemical profile in each grain given known D during peak metamorphic T. The models hold T constant at the peak value, yielding the maximum timescale that peak T conditions could persist. Timescale uncertainties for each profile were computed with Monte Carlo Bootstrap methods (Efron and Tibshirani, 1993) that take full account of uncertainties on T and diffusion coefficient calibrations.

4.2. Diffusion modelling for apatite

For apatite, we solve the one-dimensional diffusion equation

$$\frac{\partial C}{\partial t} = D(T)\frac{\partial^2 C}{\partial x^2} \quad (1)$$

using planar geometry and standard finite-difference techniques (Press et al., 1992). Because we model diffusion profiles captured within grains, no-flux boundary conditions which do not allow Sr exchange with the matrix are most appropriate. However, we also did the calculations with constant concentration boundary conditions at grain edges, and these do allow Sr exchange. Results for either case are statistically identical, indicating that the timescale estimates are dominated by internal diffusion across core-rim boundaries rather than Sr exchange with matrix phases. The initial profiles are constrained primarily by the measured concentration values and the observed (sharp BSE contrast, Fig. 2) positions of the original core-rim boundaries. The minimum number of initial step functions was specified such that the best-fit solution intersects the 2 sigma uncertainties on at least 95% of the fitted data points. In the simplest cases, initial step functions were imposed only at observed core-rim boundaries (e.g., Fig. 5D),

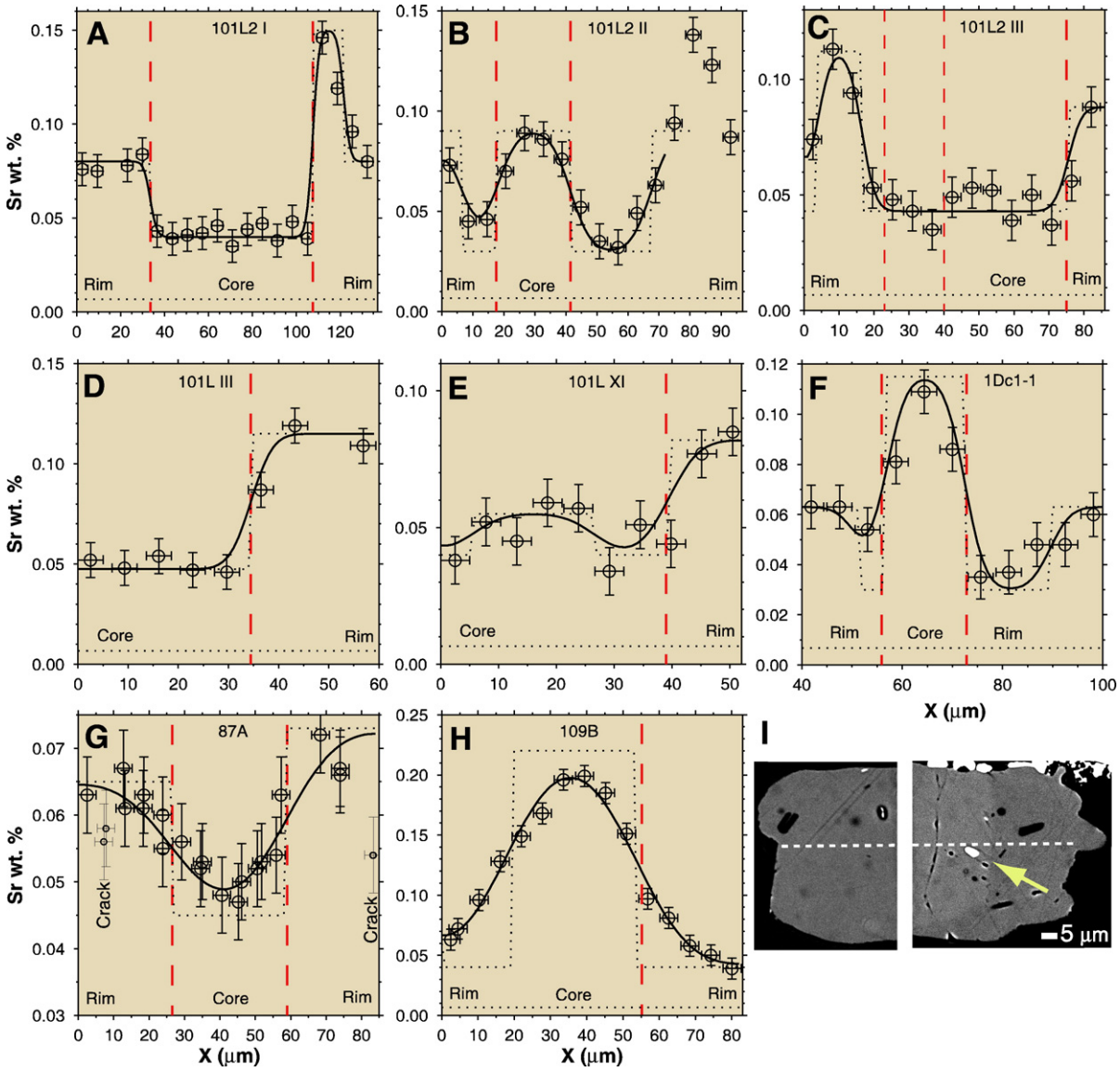

Fig. 5. (A)–(H) Sr profiles across apatite grains and diffusion modelling results. Sample numbers given at top of each graph. Error bars reflect ±2 sigma uncertainty in concentration and 5 micrometer diameter of microprobe beam spot. Detection limit for Sr denoted with horizontal dotted line. Positions of observed core–rim boundaries denoted with vertical dashed lines. Inferred step-function initial conditions denoted with dotted lines. Best-fit solutions denoted with thick black lines. A few analyses along late-stage, cross-cutting cracks in 87A were not used in the modelling. Areas of inferred growth zonation on rims of 101L2 II and 1Dc1-1 were not modelled (see text). (I) Close-up backscattered electron images of left and right margins of 109B (Fig. 5H). Core–rim boundary is clearly visible on right side (arrow). Boundary is cryptic on left side, although it may be marked by small ilmenite inclusion (bright) at very top edge of grain. Analysis profile shown with white dashed line.

but complexities in some profiles (e.g., Fig. 5C) required additional initial variation. Furthermore, for some profiles, we impose limits on lower and upper concentration values based on over two hundred apatite analyses on grains from the Bt, Grt, St, and Sil zones. The maximum Sr concentration observed was 0.22 weight percent, and the minimum, with the exception of the outermost rim of one crystal (10 μm from the edge), was 0.029 weight percent. We present sensitivity tests for the initial condition step functions and concentration values in Appendix A.

Best-fit solutions for eight apatite crystals are shown in Table 1 and Fig. 5. Uncertainties in the experimental diffusion calibration were propagated using bootstrap linear regression employing resampling of pairs or of residuals (Efron and Tibsirani, 1993) for the experimental

Table 1
Peak metamorphic timescale estimates

Sample	Metamorphic grade	Peak T (°C)	Best-fit timescale (yr) for peak T	2 sigma uncertainty range (yr)
JAB 60A	Sillimanite zone	660	1.1×10^5	1.6×10^4–5.5×10^5
JAB 62A	Sillimanite zone	660	6.8×10^4	1.9×10^5–3.1×10^4
JAB 87A	Staurolite zone	595	2.2×10^5	8.3×10^4–5.9×10^5
JAB 109 B	Staurolite zone	595	2.3×10^5	8.7×10^4–6.1×10^5
JAB 1Dc1-1	Garnet zone, near staurolite isograd	550	2.3×10^5	7.7×10^4–6.9×10^5
JAB 101L2 I	Garnet zone	535	1.6×10^5	5.0×10^4–4.8×10^5
JAB 101L2 II	Garnet zone	535	6.5×10^5	2.1×10^5–2.0×10^6
JAB 101L2 III	Garnet zone	535	2.6×10^5	8.4×10^4–8.2×10^5
JAB 101L III	Garnet zone	535	3.3×10^5	1.1×10^5–1.0×10^6
JAB 101L XI	Garnet zone	535	4.6×10^5	1.5×10^5–1.4×10^6

Sr diffusion data (Watson et al., 1985; Cherniak and Ryerson, 1993). For each candidate regression, D was calculated assuming a Gaussian error of ±30 °C about the best-estimate for T. Given the candidate D value, the time needed to produce a given measured Sr profile was estimated by solving the diffusion equation. The best-fit solution was found by minimizing chi-square (Press et al., 1992). These steps were repeated 5000 times to produce a large set of timescale estimates whose mean and standard deviation could be determined.

The bootstrap error analysis for the D of apatite uses all data (38 experimental determinations Watson et al., 1985; Cherniak and Ryerson, 1993), parallel and perpendicular to the c-axis. An extremely important aspect of the bootstrapping is that it takes full account of the covariance between the pre-exponential factor (D_o) and the activation energy (Q) in the Arrhenius expression, unlike standard error analysis which considers errors on D_o and Q independently and overestimates uncertainties on D values.

4.3. Garnet diffusion modelling

For garnet in samples JAB60A and JAB62A, we used forward modelling of radial, multicomponent diffusion in a sphere to fit the measured compositional profiles:

$$\begin{pmatrix} \frac{\partial X_1}{\partial t} \\ \frac{\partial X_2}{\partial t} \\ \frac{\partial X_3}{\partial t} \end{pmatrix} = \frac{1}{r^2}\frac{\partial}{\partial r}\left[r^2 \begin{pmatrix} D_{11} & D_{12} & D_{13} \\ D_{21} & D_{22} & D_{23} \\ D_{31} & D_{32} & D_{33} \end{pmatrix} \begin{pmatrix} \frac{\partial X_1}{\partial r} \\ \frac{\partial X_2}{\partial r} \\ \frac{\partial X_3}{\partial r} \end{pmatrix} \right] \quad (2)$$

in which X is mole fraction, r is the radius of the sphere, and the subscripts 1, 2, and 3 refer to any three of the four major components of garnet (almandine, pyrope, grossular, and spessartine). The self-diffusion coefficients were computed using the model of Carlson (Carlson, 2006), which includes the effects of unit cell dimensions, pressure, and oxygen fugacity. The elements of the diffusion coefficient matrix were then calculated using the ionic formulation of Wendt (1965), which simplifies to the following expression if the solution is near ideal or if gradients in activity coefficients are negligible (Lasaga, 1979):

$$D_{ij} = D_i^o \delta_{ij} - \left[\frac{D_i^o X_i}{\sum_{k=1}^{n} D_k^o X_k} \right] \left(D_j^o - D_n^o \right) \quad (3)$$

in which D_i^0 is the self-diffusion coefficient for component i, n is the total number of components ($n=4$), and $\delta_{ij}=0$ when $i\neq j$ and 1 when $i=j$. Diffusion in garnet has a well-documented dependence on oxygen fugacity (f_{O_2}) (Ganguly et al., 1998; Carlson, 2006). JAB60A records an f_{O_2} 2 orders of magnitude greater than the quartz-fayalite–magnetite buffer (QFM), whereas the f_{O_2} for JAB62A was 0.75 orders of magnitude below (Ague et al., 2001). High f_{O_2} can increase diffusion coefficients by an order of magnitude or more (Ganguly et al., 1998; Carlson, 2006), so the f_{O_2} variations are critical to account for, particularly because many Dalradian rocks are highly oxidized (Chinner, 1960; Ague et al., 2001).

The error analysis for garnet used 5000 Monte Carlo iterations that propagated the uncertainties on T and on the diffusion coefficient matrices. For each candidate T and set of diffusion coefficients, the best-fit solution of Eq. (2) was computed for the measured compositional profiles by minimizing chi-square. Carlson (2006) cites a general uncertainty of ±0.8 log units (95% confidence) on self-diffusion coefficients, but we found that propagating this level of uncertainty produced many "best-fit" solutions that actually fit the data poorly and showed

considerable spurious "uphill" diffusion in one or more garnet profiles. With a slightly reduced uncertainty of ±0.5 log units, however, over 99% of the candidate best-fit solutions did not show spurious large "uphill" effects; we used ±0.5 log units as the level of uncertainty for the results shown herein.

Full core–rim-profiles for the garnets studied here are presented in Baxter et al. (2002) and, for almandine, in Fig. 3. We interpret the compositional variations to be growth zoning modified to some extent by diffusion. Elemental diffusion rates were relatively fast owing to the high peak T and, for JAB60A, elevated oxygen fugacity. Garnets in lower-T greenschist or middle amphibolite facies rocks ($T < \sim 600$ °C) would have diffusion coefficients an order of magnitude or more smaller. The growth zoning in such garnets may be appropriate for modelling P–T paths and tectonic histories during garnet crystallization (Kohn, 2003), but would not be a sensitive recorder of brief thermal events that occurred after growth unless the temperature of such events was very high (upper amphibolite or granulite facies). As we document here, however, Sr diffusion in apatite is able to record brief thermal pulses under middle greenschist to middle amphibolite facies conditions, thus extending considerably the temperature range over which such pulses can be studied.

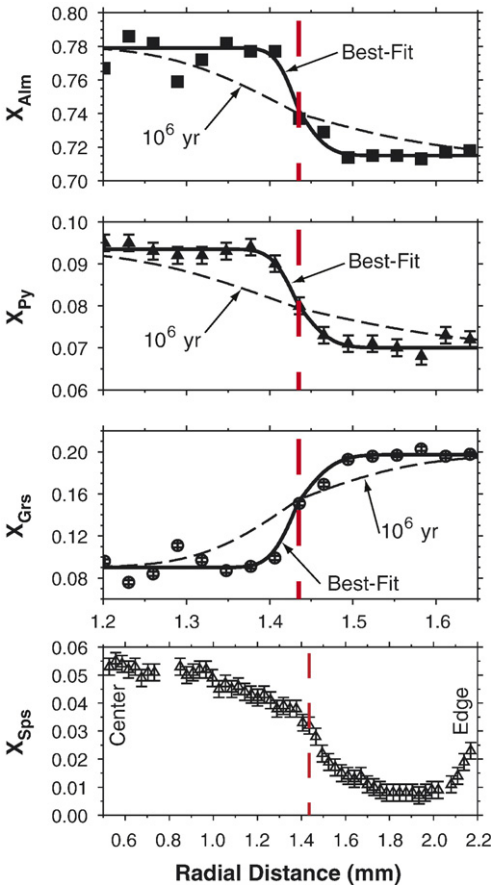

Fig. 6. Mole fraction (X) compositional profiles across Sillimanite zone garnet in JAB62A and diffusion modelling results. Vertical dashed line is garnet core–rim boundary visible in thin section. Dark solid lines represent best-fit solutions for pyrope (Py), almandine (Alm), and grossular (Grs) components based on initial step function profile (not shown for clarity). Dashed lines denote profiles after 10^6 years of diffusion. Note that the 10^6 year profiles fit the data poorly, indicating that the timescale of diffusion at peak conditions must have been considerably shorter. Spessartine (Sps) profile shows considerable growth zonation and was not fit. ±2 sigma analytical uncertainties.

The compositional profiles for each garnet are significantly different, yet yield comparable timescale estimates (Figs. 6 and 7). We used a single step function initial condition for the JAB62A profiles, corresponding to a well-defined compositional discontinuity at a radial distance of ~1.4 mm (Fig. 6). Considerable growth zonation in spessartine in JAB62A made it difficult to set initial conditions for this component, so best-fit solutions were computed based on the other three garnet components which show well-defined steps in composition at the garnet core-rim boundary (Fig. 6). Note, however, that the best-fit solution for spessartine (not shown) still gives a short timescale of only ~275,000 years, despite the uncertainties on the initial spessartine profile. The analyzed garnet in JAB60A has well-defined steps or discontinuities for the grossular, spessartine, and pyrope components at a distance of ~1.1–1.2 mm from its center (Fig. 7). We used a single step function for pyrope, and multiple step functions for the other components. The initial almandine profile at this location is less clear, so we took it as the dependent variable in the fitting. However, the almandine component shows clear oscillatory variations near the core, and these were also fit to provide a timescale estimate (Fig. 7).

5. Results and discussion

5.1. Short peak metamorphic timescales

The best-estimates for peak timescales for eight apatite (Grt and St zones) and two garnet (Sil zone) crystals are remarkably short, ranging from $< 1.0 \times 10^5$ to 6.5×10^5 yr with a geometric (logarithmic) mean of $2.3^{+1.4}_{-0.8} \times 10^5$ yr (95% confidence) or an arithmetic mean of $2.7 \times 10^5 \pm 1.3 \times 10^5$ yr (Table 1, Fig. 8). Notably, the timescales agree regardless of metamorphic grade, at least within our uncertainties. The results for apatite and garnet are statistically indistinguishable, although there is a suggestion that the peak timescales may decrease with increasing

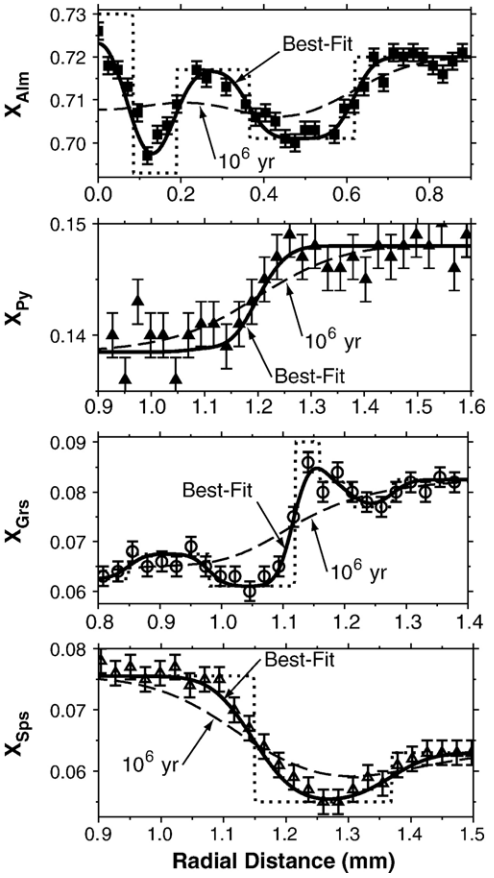

Fig. 7. Mole fraction (X) compositional profiles across Sillimanite zone garnet in JAB60A and diffusion modelling results. Dark solid lines represent best-fit solutions. Single step function initial conditions for Py not shown for clarity; multiple step function initial conditions for Alm and Sps shown with dotted lines. Dashed lines denote profiles after 10^6 years of diffusion. Note that the 10^6 year profiles fit the data poorly, indicating that the timescale of diffusion at peak conditions must have been considerably shorter. ±2 sigma analytical uncertainties.

grade (garnet diffusion modelling produced the shortest timescales). The results indicate that the crystals-and the rocks that contain them-were held at peak temperatures for extremely short timescales of <1 million years duration. For apatite, the diffusion expression of Cherniak and Ryerson (1993) yields a characteristic length scale $2\sqrt{Dt}$ of ~80 micrometers at peak Sil zone T of 660 °C for 300,000 years, enough to homogenize typical apatite crystals observed in this study (Fig. 3).

Our calculated timescales are maximum values for the following reasons. First, the calibration we use is for "dry" systems (Watson et al., 1985; Cherniak and Ryerson, 1993). There is some evidence that water may increase Sr diffusion rates in apatite at $T<\sim 750$ °C (Farver and Giletti, 1989; Cherniak and Ryerson, 1993). While the latter point may be controversial, the presence of water will certainly not decrease Sr diffusivity (Cherniak and Ryerson, 1993; Watson and Baxter, 2007). Second, given uncertainties in the orientations of the measured crystals, we use a planar geometry for diffusion modelling. Two-dimensional effects decrease peak timescale estimates; cylindrical and spherical models typically reduce timescales by 5–10%. Third, we used Monte Carlo methods to investigate a wide range of other potential initial conditions besides simple step functions for representative profiles as described in the Appendix. For each profile, over 99% of the potential initial conditions produced shorter timescale estimates and/or poorer fits to the data. Thus, simple step functions provide the best fit and the most conservative (longest) timescale estimates. Finally, we used the largest grains in each sample in an effort to obtain central sections through crystals. Aliasing of profiles due to off-center analyses would tend to overestimate timescales.

There has been some controversy over the diffusivity of Ca in garnet such that its diffusion coefficient may be much smaller than those for other elements (Vielzeuf et al., 2007). However, our results do not reveal any inconsistencies between the various components, which suggests that the calibration of Carlson (2006) is fully

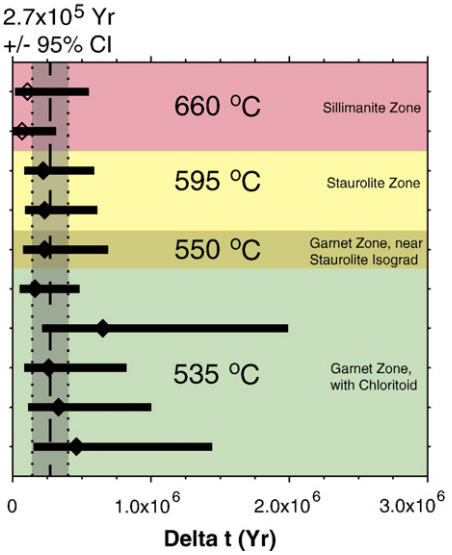

Fig. 8. Average total timescale for peak thermal conditions (Delta t) is 2.7×10^5 yr; 95% confidence limits (CI) shown with vertical gray bar. Mean for each individual apatite grain shown with filled diamond, and ±2 sigma limits shown with horizontal black bar. The geometric mean was used to account for the long "tail" of the distributions toward longer timescales resulting from the exponential term in the Arrhenius relationship. The Sil zone results are average values and uncertainty ranges for multicomponent diffusion in garnet from samples JAB60A and JAB62A.

internally consistent. Even if the diffusion coefficient for Ca is arbitrarily decreased by an additional factor of 5, best-fit timescales for all garnet components remain brief (<200,000 yr for most cases; ~400,000 yr maximum).

The brevity of peak conditions may account for the widespread presence of relict kyanite in the Sil zone rocks of Glen Clova (Chinner, 1960; Ague et al., 2001). Given the well-known sluggishness of reactions among the Al_2SiO_5 polymorphs, it is likely that the high-T conditions simply did not last long enough to allow conversion of all the kyanite to sillimanite.

5.2. Diffusion versus recrystallization

Some studies have documented fluid-induced recrystallization of apatite and other phosphates which would affect diffusion modeling (Harlov et al., 2005; Villa, 2006). Indeed, we call upon apatite neocrystallization to produce the initial, pre-peak, core-rim step profiles we observe. However, it is extremely unlikely that the smoothed chemical profiles we measured in both apatite and garnet are due to recrystallization *after* the peak of metamorphism, as described here.

First, it is difficult to conceive how post-peak recrystallization would somehow provide the same timescale estimate over several metamorphic zones for both apatite and garnet. Varying amounts of recrystallization driven by spatially and temporally fluctuating phenomena including fluid infiltration or deformation would not be expected to produce any systematic timescale estimates from sample to sample, from apatite to garnet, or across all metamorphic grades. On the other hand, diffusion within existing grains in response to a pulsed thermal event would be expected to produce consistent profiles and timescale estimates such as we observe.

Second, the core of one of the garnets we study (62A) is a lower-grade relict that lacks sillimanite inclusions. The rim contains sillimanite zone inclusions and grew during amphibolite facies metamorphism, as dated by Sm/Nd (Baxter et al., 2002). Sm/Nd dating of the other garnet (60A), which lacks any aluminosilicate inclusions, demonstrates that it grew prior to peak metamorphism (i.e. prior to garnet 62A rim) and must, therefore, have undergone Sil zone conditions (Baxter et al., 2002).

Third, garnet is highly refractory, so the chemical profiles we measure inside the crystals must reflect growth zonation modified to some extent by diffusion, rather than post-peak recrystallization.

Fourth, the apatite crystals are elongate parallel to the main foliation in the rocks. Truncated detrital cores and overgrowths parallel to the foliation (Fig. 2) are consistent with simultaneous pressure solution of cores at high stress areas perpendicular to foliation, and reprecipitation in low stress areas parallel to foliation. Refractory metamorphic porphyroblasts such as plagioclase, garnet, chloritoid, and staurolite contain apatite crystals that display similar asymmetric core-rim textures, so the apatites and their textures must pre-date the peak (though see below). Apatite grains included within garnet (e.g., 101L III) give timescale estimates that are statistically identical to matrix grains (e.g., 101L2 III).

While it is conceivable that retrograde fluids may have accessed some apatite grains via cracks within porphyroblasts, we observe few such cracks in 2-D thin sections, and alteration of included apatites would not produce the same asymmetric recrystallization pattern that we observe. In addition, if apatites did recrystallize during some lower temperature retrograde fluid infiltration event, we would expect to see a chemically homogeneous rim with no diffusive modification. Furthermore, although isolated patches of retrograde chlorite are observed in a few samples, the apatites are not texturally related to the chlorite and are instead found in contact with fresh, peak metamorphic minerals or mineral assemblages.

As discussed above, core–rim textures were not observed in our Sil zone apatite samples, presumably because such textures were eliminated by rapid diffusion at high T. Importantly, however, the Sil zone garnets provide independent constraints on peak timescales.

Finally, pressure solution of apatite parallel to foliation after peak metamorphism is not a viable hypothesis. The apatites we measured lie parallel to the dominant foliation in the rocks, and this foliation is overgrown by, and is therefore older than, peak porphyroblasts. Apatite crystals that formed after the peak would be expected to randomly overgrow the foliation, not be elongate parallel to it as observed in the rocks.

5.3. Temperature-time histories

By modelling diffusion with peak T conditions, we ignore the time (and diffusive exchange) that would occur during the non-zero duration of temperature increase and decrease from below 500 °C to the peak. Given the slow Sr diffusion in apatite below 500 °C, these effects are negligible, but including them nevertheless only decreases the peak metamorphic timescale. However, while we don't know in detail the shape (in T-time space) of the thermal pulse (or pulses), the diffusion modelling allows us to constrain the total time-integrated amount of diffusion for each profile using: $L^2 = \langle Dt \rangle$ where L is the characteristic diffusion length scale indicated by the data. The time-integrated $\langle Dt \rangle$ is uniquely constrained by the measured data. Even in

models including more complex heating and cooling, or multiple pulses, the <*Dt*> constrains the total timescale for which conditions above ~500 °C persisted to be less than <1 myr in all cases (Fig. 9).

5.4. Comparison with other studies of diffusion in the Dalradian

Two other studies examine qualitatively diffusion in Dalradian garnets, both of which argue for long >1 Myr timescales in apparent conflict with our new results (Dempster, 1985; Ayres and Vance, 1997). One study (Ayres and Vance, 1997) uses modal, bulk rock chemical, and electron microprobe data from the paper of Atherton (1968) to reconstruct hypothetical initial Mn profiles for three garnets based on Rayleigh fractionation. These profiles were then relaxed with a diffusion model to provide qualitative timescale information. However, the Mn contents of other Mn-bearing minerals in the rocks (including chlorite, epidote group minerals, and oxides) were not accounted for when the hypothetical profiles were constructed, nor were the garnet growth histories. Growth histories are important because the Mn contents of garnets can vary widely even in a single rock sample due to variations in the timing of nucleation (Chernoff and Carlson, 1997). For both of these reasons, the initial Mn profiles needed for diffusion modelling are not tightly constrained and cannot be used to estimate timescales. Furthermore, one of the three garnets is from the Grt zone (sample 5) and would not be expected to have undergone large amounts of diffusion (due to the relatively low *T*), and another (sample 7) may have been affected by the contact aureole of the Dunfallandy Hill Granite. The third garnet (sample 13) does come from the regional staurolite–kyanite zone, although these metamorphic conditions were lower-*T* than the Sil zone we consider. This rock contains nearly 11 modal percent epidote group minerals which can host significant Mn (particularly under relatively oxidizing conditions), but epidote was not considered when selecting the distribution coefficient needed to reconstruct the hypothetical initial profiles. Elevated oxygen fugacity is likely given the relatively high Fe_2O_3/FeO ratio of the bulk rock (Chinner, 1960; Atherton, 1968; Ague et al., 2001). We note that Atherton (1968) fit the measured profiles reasonably well using a simple model of Mn fractionation during growth that required no diffusional modification.

The other paper examines several Sil zone garnets (Dempster, 1985). One of these clearly retains growth zoning, whereas two others have relatively flat, smooth compositional profiles. It is critical to place garnet growth in context because garnets grew during both Grt zone and Sil zone conditions (McLellan, 1985; Ague et al., 2001). Without such context, it is not possible to evaluate the zoning profiles in great detail. Although it is asserted that Sil zone garnets could have been largely homogenized by diffusion, our measured profiles clearly show that major compositional heterogeneities were able to persist in the Sil zone (Figs. 3, 6, 7). One possibility is that the relatively smooth profiles for two of the garnets reflect growth at Sil zone conditions. Another possibility is that Sil zone temperatures were locally higher than those of Glen Clova, and were thus sufficient to homogenize

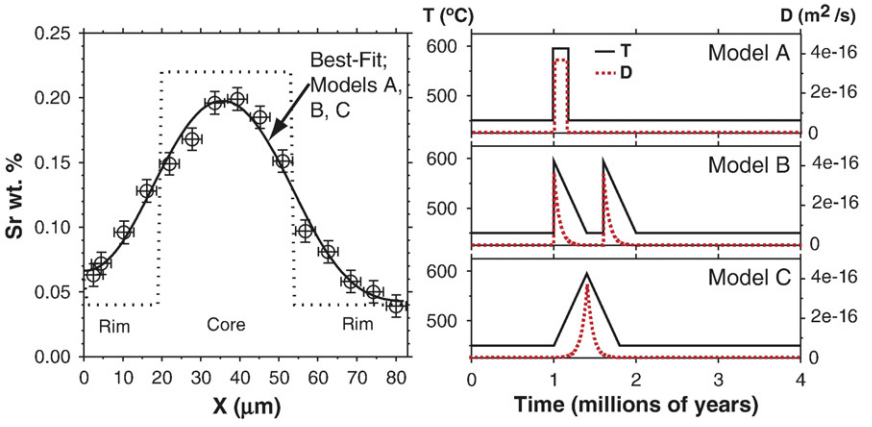

Fig. 9. Diffusion modelling results for more complex thermal histories. The example is an apatite diffusion profile from the Staurolite zone (Figs. 3 and 5). The best fit diffusion model is consistent with each of the Model thermal histories (A,B,C) shown, each constrained by the fact that the total $L = \text{sqrt}\langle Dt \rangle$ indicated by this profile is 7.5×10^{-6} m (where <*Dt*> is the area under the dashed lines in each model). Model A was used in calculations presented in Fig. 8. In Model B, our data alone do not constrain the time gap between pulses during which essentially no diffusion will occur. However, geochronologic constraints (Baxter et al., 2002) limit the maximum span of peak metamorphic conditions to within a few million years.

garnet compositions. New T and oxygen fugacity estimates that take into account non-ideal mixing in silicates and oxides are required to evaluate the possible impact of regional peak temperature variations on diffusion in Sil zone garnets.

As shown in Figs. 6 and 7, it is clear that timescales of peak heating of 1 million years or more would have resulted in considerable smoothing of garnet profiles and could not have preserved the short wavelength compositional variations that we measure at Glen Clova. The short timescales from garnet modelling corroborate the results from apatite modelling.

6. Petrological and tectonic implications of extremely brief thermal pulses

The Grampian orogeny lasted for only c. 10–15 Ma in Scotland (Friedrch et al., 1999; Oliver et al., 2000; Baxter et al., 2002) and probably involved subduction along the Highland Boundary Fault (Dempster et al., 2000; Masters and Ague, 2005). While a background (i.e.,< ~ 500 °C) regional conductive heating and cooling due to overthickening probably spanned nearly the entire 10–15 Ma orogeny, the thermal peak conditions lasted for only 200–300 kyr and were attained c. 465 Ma close to the end of the orogeny (Fig. 10). The peak heating could have occurred in one pulse, or in a series of shorter ones that integrate to several hundred thousand years (Fig. 9) but were spread out over no more than a few myr

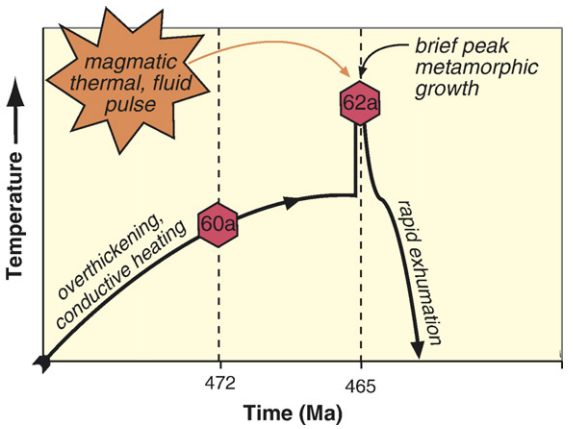

Fig. 10. Cartoon of inferred metamorphic history based on age relations at Glen Clova. Peak thermal pulse, dated at c. 465 Ma by Sm/Nd garnet dating of JAB62A (Baxter et al., 2002) occurs near the end of the 10–15 Ma orogenic cycle. Earlier garnet growth occurred in the greenschist facies before the peak, as evidenced by Sm/Nd dating of JAB60A (Baxter et al., 2002) and Sm/Nd garnet dating elsewhere in the Dalradian (Oliver et al., 2000; Baxter et al., 2002). Rapid exhumation is based on Dalradian age garnets in c. 465 Ma sediments (Oliver et al., 2000).

(Oliver et al., 2000; Baxter et al., 2002). This pulsed peak heating produced the classic Barrovian sequence in the northeastern Highlands, and probably the Buchan sequence to the north as well (Oliver et al., 2000). Brief episodes of heating and related metamorphic reactions interspersed with longer intervals of relative quiescence could help explain measurements of slow time-integrated reaction rates in general (van Haren et al., 1996; Baxter and DePaolo, 2000; Baxter, 2003).

The thermal energy may have been supplied by magmas and associated fluid flow (Baxter et al., 2002), and/or related to shear heating associated with regional extension (Viete et al., 2006). An advective heat component is supported by the observations that: 1) the metamorphic peak was synchronous with the intrusion of several large magma bodies (Baxter et al., 2002) (Fig. 1) and with large regional fluid fluxes (Breeding et al., 2004; Masters and Ague, 2005); and 2) peak T values in the Grt through Sil zones were attained penecontemporaneously (Baxter et al., 2002). A critical point to emphasize in this regard is that the high-grade amphibolite facies rocks developed only in the northeastern part of the Dalradian where syn-Barrovian magmatism occurred, and are rare or absent to the southwest where such magmatism is lacking. Our model is similar in some respects to that advanced by Lux et al. (Lux et al., 1986) to explain low-pressure/high-temperature metamorphic heating in New England, but we note that these authors did not focus on constraining the timescales of such heating. Additionally, Chamberlain and Rumble (1989) argue that regional metamorphic "hot spots" in New England (peak T=650–750 °C), and consequent steep thermal gradients in surrounding rocks (dropping to ~500 °C within a few km) could only have been produced by a rapid c. 100,000 yr pulse of focused, hot fluids. While the geometries and fluid flow paths in Scotland are not fully constrained, our data suggest a similarly short pulse of heat creating similar peak temperatures (~660 °C) above a similar background conductive thermal maximum (~500 °C). Large fluid fluxes (Chamberlain and Rumble, 1989; Breeding et al., 2004; Masters and Ague, 2005), in concert with magmatism, could have been rapid and efficient carriers of heat.

The rapid cooling implied by the short thermal peak timescale was probably related to exhumation. Detrital Dalradian garnet that has the peak metamorphic age (c. 465 Ma) is found in the 465±2.5 Ma sediments of the Southern Uplands (Oliver et al., 2000). The overlap of the metamorphic age and the sedimentary age indicates that exhumation was rapid and could, therefore, have truncated the timescale of peak thermal conditions. For

the 0.4–0.6 GPa pressures of metamorphism, fast "plate tectonic" exhumation rates approaching a centimeter per year or more are implied (Oliver et al., 2000). Models that relate exhumation to regional compression (Oliver et al., 2000) or extension (Viete et al., 2006) have been proposed. Cooling may also have been aided by fluid flow from the cooler flanks of the orogen into the higher-T zones; geochemical evidence consistent with such flow has been recognized in the Dalradian (Ague, 1997; Breeding et al., 2004; Masters and Ague, 2005).

We conclude that the classic progression of isograds in the Barrovian type locality developed in response to geologically short ($<10^6$ yr) peak heating at the regional scale, and that such short metamorphic pulses may exert the dominant control on mineralogy and rock type sequences in mountain belts.

Acknowledgements

We thank J.O. Eckert, Jr., for valuable assistance with the electron microprobe, A. Camacho for thoughtful comments on an earlier version of this paper, two anonymous referees for their critical and constructive reviews, and the National Science Foundation Directorate for Geosciences for support (NSF EAR-0509934 to JJA and EAR-0547999 to EFB).

Appendix A. Sensitivity tests of initial conditions

A.1. Tests of step functions

We tested other initial concentration profiles besides simple step functions for apatite. We took two representative profiles (101L III, 101L2 I), and generated a wide range of model initial profiles using Monte Carlo methods. These were: a) 2, 3, 4, and 5 equally-spaced, random step functions across the core-rim boundary; b) 2, 3, and 4 equally-spaced, random (but connected) lines across the boundary; and c) random concentration values at 1 μm intervals across the boundary. In all cases, the upper and lower limits on the randomly-selected Sr concentrations were set by the Sr values measured outside the boundary region, with an additional generous allowance for 3 sigma errors in measured concentration.

Each model initial condition was subjected to the chi-square fitting procedures described above; the fit was then compared to that obtained using simple step functions. Some 40,000 model diffusion profiles were evaluated, with the result that over 99% of the model results either gave a *shorter* timescale or a *poorer* fit relative to the initial condition of simple step functions. For example, for 101L III, only 0.5% of the trials fit better (smaller chi-square) and yielded a longer timescale. Importantly, however, the average of these few longer timescale results was 410,000 years, insignificantly different than the estimate of 330,000 years obtained with a simple step function. Simple step functions are also qualitatively most consistent with the relatively abrupt core-rim boundaries observed in backscattered electron images (Fig. 2).

A.2. Initial Sr concentration values

The concentration values used for the initial step function profiles also deserve comment. Sharp core-rim transitions, such as those found in 101L III and 101L2 I, are very straightforward to model (Figs. 5A,D). Others require additional considerations. For example, for 1Dc1-1, we impose the minimum Sr concentration of 0.03 weight percent discussed in Section 4.2 (Fig. 5F). One might argue that the maximum Sr value in the core is unconstrained and could have thus been larger; this would yield a longer timescale estimate. Increasing Sr in the core arbitrarily to a large value (0.18 weight percent), yields an extremely poor fit to the data (curve I in Fig. A1A) with chi-square 12 times greater (poorer) than the preferred best-fit. The profile could be fit better with this large Sr concentration value if the core region was much narrower, but this is untenable based on the observed positions of the original core-rim boundaries and the symmetry of diffusion (Figs. 2 and 5F). One might also suggest that the minimum concentration should be zero (although all analyzed apatites had Sr concentrations above detection limits). In this case, the Sr concentration in the core would need to be increased by 0.03 weight percent to preserve the symmetry of the profile. With these initial conditions, the fit shown by curve II in Fig. A1A remains noticeably poorer than our preferred best-fit solution (chi-square 2.5 times larger).

In the profile for 87A (Fig. 5G), it could be suggested that both the initial minimum and maximum concentrations should be different than our preferred estimates. Regardless, the position and width of the low Sr core is tightly constrained by the observed core-rim boundaries. One could decrease the core Sr concentration to the minimum constraint value of 0.03 weight percent, and increase the initial rim values to maintain the overall symmetry of the fit. Even with these very conservative assumptions, the time scale estimate is within the 2 sigma uncertainties of our calculations based on our preferred initial condition.

Similar reasoning applies to the 109B profile (Fig. H). Decreasing the minimum concentration to 0.03 weight percent and increasing the maximum accordingly results

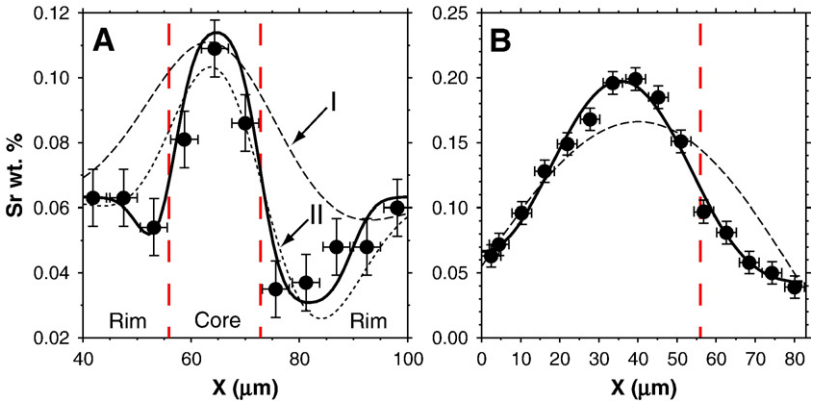

Fig. A1. Tests of initial concentration values used in modelling. Solid lines are preferred best-fit solutions. Positions of observed core–rim boundaries shown with dashed vertical lines. (A) Results for profile 1Dc1-1. Fits I and II described in Appendix denoted with dashed lines. Note that neither I nor II corresponds to the data as well as the best-fit solution. (B) Results for profile 109B. Dashed line denotes alternative fit described in Appendix; note that it fits the data poorly and has the wrong overall shape.

in only a small difference in the timescale estimate (~50,000 years). In addition, we note that the initial Sr concentration in the core for the best-fit solution is already at the maximum value observed for any sample at any metamorphic grade. One could take an extreme position and assume that the concentration of Sr was initially high and uniform across the crystal, and that Sr was lost by diffusion to the matrix at the edges of the crystal. This scenario assumes that there was no initial concentration difference across the core-rim boundary, and is thus highly unlikely. Nonetheless, in Fig. A1B we show the results for diffusion obtained by setting the initial Sr concentration to 0.22 wt.% across the grain, with fixed, time-invariant Sr concentrations at the crystal edges. The minimum chi-square fit is clearly poor and, significantly, it has the wrong shape, being everywhere convex upward. This shape is characteristic for profiles dominated by diffusive loss to the surroundings, and is clearly inappropriate here.

The profile shown in Fig. 5B has what we infer to be growth zonation on its left and right margins. We did not fit the right part of the profile because of uncertainties on the initial condition. It could be argued that this part of the profile was impacted by diffusion as well as growth. It is critical to emphasize in this regard that the wavelength of this zonation feature is the same as that observed for diffusion-related zoning directly at the core-rim boundaries. So even if the feature was diffusion-related, the timescales would be comparable to the rest of the profile by simple $\sqrt{Dt}$ arguments. The lower concentration bounds were set at the 0.03 weight percent minimum. This fixes the maximum concentration, because symmetry must be preserved relative to the core-rim boundaries. Arbitrarily increasing the maximum concentration in the core to a larger value results in much poorer fits to the data, analogous to the results shown for curve I in Fig. A1A.

The concentration of Sr in the core of 101L XI fluctuates somewhat, but clearly has an average value of about 0.045 wt.% (Fig. 5E). Arbitrarily increasing the initial concentration in the rim simply results in poorer fits. For example, increasing the rim concentration to 0.1 or 0.15 wt.% increases chi-square by more than a factor of two or seven, respectively, relative to the best-fit value. Similar considerations apply for profile 101L2 III (Fig. 5C).

Appendix B. Supplementary data

Supplementary data associated with this article can be found, in the online version, at doi:10.1016/j.epsl.2007.07.017.

References

Ague, J.J., 1997. Crustal mass transfer and index mineral growth in Barrow's garnet zone, northeast Scotland. Geology 25, 73–76.

Ague, J.J., Baxter, E.F., Eckert Jr., J.O., 2001. High f_{O_2} during sillimanite zone metamorphism of part of the Barrovian type locality, Scotland. J. Petrol. 42, 1301–1320.

Atherton, M.P., 1968. The variation in garnet, biotite, and chlorite composition in medium grade pelitic rocks from the Dalradian, Scotland, with particular reference to zoning in garnet. Contrib. Mineral. Petrol. 18, 347–371.

Atherton, M.P., 1977. The metamorphism of the Dalradian rocks of Scotland. Scott. J. Geol. 13, 331–370.

Ayres, M., Vance, D., 1997. A comparative study of diffusion profiles in Himalayan and Dalradian garnets: constraints on diffusion data and the relative duration of the metamorphic events. Contrib. Mineral. Petrol. 128, 66–80.

Barrow, G., 1893. On an intrusion of muscovite–biotite gneiss in the south-eastern highlands of Scotland, and its accompanying metamorphism. Q. J. Geol. Soc. Lond. 49, 330–354.

Baxter, E.F., 2003. Natural constraints on metamorphic reaction rates. In: Vance, D., Muller, W., Villa, I.M. (Eds.), Geochronology-linking the Isotopic Record with Petrology and Textures. J. Soc. Lond. Spec. Pub., vol. 220, pp. 183–202.

Baxter, E.F., DePaolo, D.J., 2000. Field measurement of slow metamorphic reaction rates at temperatures of 500° to 600 °C. Science 288, 1411–1414.

Baxter, E.F., Ague, J.J., DePaolo, D.J., 2002. Prograde temperature–time evolution in the Barrovian type-locality constrained by Sm/Nd garnet ages from Glen Clova, Scotland. J. Geol. Soc. Lond. 159, 71–82.

Bjornerud, M.G., Austrheim, H., 2006. Hot fluids or rock in eclogite facies metamorphism? Nature 440, E4.

Breeding, C.M., Ague, J.J., Grove, M., Rupke, A., 2004. Isotopic and chemical alteration of zircon by metamorphic fluids; U–Pb age depth-profiling of zircons from Barrow's garnet zone, northeast Scotland. Am. Mineral. 89, 1067–1077.

Camacho, A., Lee, J.K.W., Hensen, B.J., Braun, J., 2005. Short-lived orogenic cycles and the eclogitization of cold crust by spasmodic hot fluids. Nature 435, 1191–1196.

Carlson, W.D., 2006. Rates of Fe, Mg, Mn, and Ca diffusion in garnet. Am. Mineral. 91, 1–11.

Carlson, W.D., Schwarze, E., 1997. Petrological significance of homogenization of prograde growth zoning in garnet; an example from the Llano uplift. J. Metamorph. Geol. 15, 631–644.

Chamberlain, C.P., Rumble III, D., 1988. Thermal anomalies in a regional metamorphic terrane: An isotopic study of the role of fluids. J. Petrol. 29, 1215–1232.

Chamberlain, C.P., Rumble III, D., 1989. The influence of fluids on the thermal history of a metamorphic terrain: New Hampshire, USA. In: Daly, J.S., Cliff, R.A., Yardley, B.W.D. (Eds.), Evolution of Metamorphic Belts. Geological Society Special Publication, vol. 43. Blackwell, Oxford, pp. 203–213.

Cherniak, D.J., Ryerson, F.J., 1993. A study of strontium diffusion in apatite using Rutherford backscattering spectroscopy and ion implantation. Geochim. Cosmochim. Acta 57, 4653–4662.

Chernoff, C.B., Carlson, W.D., 1997. Disequilibrium for Ca during growth of pelitic garnet. J. Metamorph. Geol. 15, 421–438.

Chinner, G.A., 1960. Pelitic gneisses with varying ferrous/ferric ratios from Glen Clova, Angus, Scotland. J. Petrol. 1, 178–217.

Dachs, E., Proyer, A., 2002. Constraints on the duration of prograde metamorphism in the Tauern Window from diffusion modelling of discontinuous growth zones in eclogite garnet. J. Metamorph. Geol. 20, 769–780.

Dempster, T.J., 1985. Garnet zoning and metamorphism of the Barrovian type area, Scotland. Contrib. Mineral. Petrol. 89, 30–38.

Dempster, T.J., Fallick, A.E., Whittemore, C.J., 2000. Metamorphic reactions in the biotite zone, eastern Scotland: high thermal gradients, metasomatism, and cleavage formation. Contrib. Mineral. Petrol. 138, 348–363.

Efron, B., Tibshirani, R.J., 1993. An Introduction to the Bootstrap. Chapman and Hall, New York.

Farver, J.R., Giletti, B.J., 1989. Oxygen and strontium diffusion kinetics in apatite and potential applications to thermal history determinations. Geochim. Cosmochim. Acta 53, 1621–1631.

Faryad, S.W., Chakraborty, S., 2005. Duration of Eo-Alpine metamorphic events obtained from multicomponent diffusion modeling of garnet: a case study from the eastern Alps. Contrib. Mineral. Petrol. 150, 306–318.

Friedrch, A.M., Hodges, K.V., Bowring, S.A., Martin, M.W., 1999. Short-lived continental magmatic arc at Connemara, western Irish Caledonides: implications for the age of the Grampian orogeny. Geology 27, 27–30.

Ganguly, J., Chakraborty, S., Sharp, T.G., Rumble III, D., 1996. Constraint on the time scale of biotite-grade metamorphism during Acadian orogeny from a natural garnet–garnet diffusion couple. Am. Mineral. 81, 1208–1216.

Ganguly, J., Cheng, W., Chakraborty, S., 1998. Cation diffusion in aluminosilicate garnets: experimental determinations in pyrope–almandine diffusion couples. Contrib. Mineral. Petrol. 131, 171–180.

Graham, C.M., Valley, J.W., Eiler, J.M., Wada, H., 1998. Timescales and mechanisms of fluid infiltration in a marble: an ion microprobe study. Contrib. Mineral. Petrol. 132, 371–389.

Harlov, D.E., Wirth, R., Forster, H.J., 2005. An experimental study of dissolution–reprecipitation in fluorapatite: fluid infiltration and the formation of monazite. Contrib. Mineral. Petrol. 150, 268–286.

Kelly, S., 2005. Hot fluids and cold crusts. Nature 435, 1171.

Kohn, M.J., 2003. Geochemical zoning in metamorphic minerals, in: Rudnick, R.L. (Ed.), The Crust. Treatise on Geochemistry (Holland, H.D., Turekian, K.K., Eds.), Elsevier-Pergamon, Oxford, pp. 229–261.

Lasaga, A.C., 1979. Multicomponent exchange and diffusion in silicates. Geochim. Cosmochim. Acta 43, 455–469.

Lasaga, A.C., Jiang, J., 1995. Thermal history of rocks; P–T–t paths for geospeedometry, petrologic data, and inverse theory techniques. Am. J. Sci. 295, 697–741.

Lawson, C.L., Hanson, R.J., 1974. Solving Least Squares Problems. Prentice-Hall, Englewood Cliffs.

Lux, D.R., DeYoreo, J.J., Guidotti, C.V., Decker, E.R., 1986. Role of plutonism in low-pressure metamorphic belt formation. Nature 323, 794–797.

Masters, R.L., Ague, J.J., 2005. Regional-scale fluid flow and element mobility in Barrow's metamorphic zones, Stonehaven, Scotland. Contrib. Mineral. Petrol. 150, 1–18.

Masters, R.L., Ague, J.J., Rye, D.M., 2000. An oxygen and carbon isotopic study of multiple episodes of fluid flow in the Dalradian and Highland Border Complex, Stonehaven, Scotland. J. Geol. Soc. Lond. 157, 367–379.

McLellan, E.L., 1985. Metamorphic reactions in the kyanite and sillimanite zones of the Barrovian type area. J. Petrol. 26, 789–818.

Oliver, G.J.H., Chen, F., Buchwaldt, R., Hegner, E., 2000. Fast tectonometmorphism and exhumation in the type area of the Barrovian and Buchan zones. Geology 28, 459–462.

Press, W.H., Teukolsky, S.A., Vetterling, W.T., Flannery, B.P., 1992. Numerical Recipes in FORTRAN, second ed. Cambridge University Press, Cambridge.

Thompson, A.B., England, P.C., 1984. Pressure–temperature–time paths of regional metamorphism II, their inference and interpretation using mineral assemblages in metamorphic rocks. J. Petrol. 25, 929–955.

van Haren, J.L.M., Ague, J.J., Rye, D.M., 1996. Oxygen isotope record of fluid infiltration and mass transfer during regional metamorphism of pelitic schist, south-central Connecticut, USA. Geochim. Cosmochim. Acta. 60, 3487–3504.

Vielzeuf, D., Baronnet, A., Perchuk, A.L., Laporte, D., Baker, M.B., 2007. Calcium diffusivity in alumino-silicate garnets: an experimental and ATEM study. Contrib. Mineral. Petrol. 154, 153–170.

Viete, D.R., Richards, S.W., Lister, G.S., 2006. Time-scales and heat sources for Barrovian regional metamorphism. Goldschmidt Conference, 16th, Melbourne, Australia.

Villa, I.M., 2006. From nanometer to megameter: Isotopes, atomic-scale processes, and continent-scale tectonic models. Lithos 87, 155–173.

Watson, E.B., Baxter, E.F., 2007. Diffusion in solid-earth systems. Earth Planet. Sci. Lett. 253, 307–327.

Watson, E.B., Harrison, T.M., Ryerson, F.J., 1985. Diffusion of Sm, Sr, and Pb in fluorapatite. Geochim. Cosmochim. Acta 49, 1813–1823.

Weber, W.J., Ewing, R.C., Meldrum, A., 1997. The kinetics of alpha-decay-induced amorphization of zircon and apatite containing weapons-grade plutonium and other actinides. J. Nucl. Mater. 250, 147–155.

Wendt, R.P., 1965. The estimation of diffusion coefficients for ternary systems of strong and weak electrolytes. J. Phys. Chem. 69, 1227–1237.

Wijbrans, J.R., McDougall, I., 1986. $^{40}Ar/^{39}Ar$ dating of white micas from an Alpine high-pressure metamorphic belt on Naxos, Greece: the resetting of the argon isotopic system. Contrib. Mineral. Petrol. 93, 187–194.

Wilbur, D.E., Ague, J.J., 2006. Chemical disequilibrium during garnet growth: Monte Carlo simulations of natural crystal morphologies. Geology 34, 689–692.